RSC Advances

ROYAL SOCIETY OF CHEMISTRY

www.rsc.org/advances

Cite this: DOI: 10.1039/c0xx00000x

www.rsc.org/xxxxxx

ARTICLE TYPE

Neurotoxin-Directed Synthesis and In Vitro Evaluation of Au Nanoclusters

Zhengbo Sun[a], Wenlu Zhang[a], Pengfei Zhang[a], Duyang Gao[a], Ping Gong[a], Xue-Feng Yu[a*], Yingliang Wu[b], Zhijian Cao[b], Wenxin Li[b*], Lintao Cai[a*]

Multifunctional theranostic materials with good biocompatibility are the desired features of cancer imaging and therapy. In this paper, a glioma-specific theranostic agent is prepared by using Chlorotoxin fusion protein GST-CTX (gCTX) as a template to direct the synthesis of Au nanoclusters (NCs). By trapping the Au NCs in the gCTX, the prepared Au@gCTX NCs show ultrasmall size with hydrodynamic diameter of ~2.2 nm and exhibit red-emitting fluorescence with quantum yield of approximately 6.5%.The investigation from confocal fluorescent microscopy reveals the bright fluorescence and high specificity of the Au@gCTX NCs to label glioma cells through binding to membrane-bound matrix metalloproteinase 2 (MMP-2). Gelatin Zymography, MTT cell viability assay and flow cytometry studies further exhibit that the Au@gCTX NCs can inhibit the enzymatic activity of MMP-2 and cancer proliferation by elevating intracellular ROS levels, and without harmful to normal cells. Our results suggest an efficient method for the synthesis of multifunctional theranostic agent for the treatment of cancer.

Introduction

Gliomas are currently the most common and lethal type of primary brain tumor for which effective diagnostics and treatment strategies are currently lacking. Because of the poor visual contrast between neoplastic and normal brain tissue, the effectiveness of tumor resection in neurosurgery is severely limited.[1] Although there are some advances in chemo and radiation therapy regimens, the median survival of glioma patients has been unaltered in the last 20 years.[2] In recent years, cancer treatment which combines medical imaging and targeted therapy in a single entity has drawn strong interest and much attention.[3] Considerable efforts have been directed towards the fabrication of theranostic agents based on various nanomaterials such as quantum dots, magnetic nanoparticles, and plasmonic nanoparticles, etc.[4-7] These nanoscale theranostic agents have the potential to integrate the tumor detection and treatment, and enable real-time visualization of therapeutic biodistribution. However, much more work needs to be done to combat the inherent toxicity of these nanoscale agents before translation into clinical use. In addition, the agents with large size (over 20 nm) often suffer from high reticuloendothelial system (RES) uptake, which may reduce their efficiency and sensitivity.[7] Therefore, there is still a great demand for small and biocompatible theranostic agents to achieve the combination of cancer imaging and therapy.

Chlorotoxin (CTX), a widely studied peptide neurotoxin, has been proven to be a highly efficient glioma targeting molecule for both tumor labeling and therapy. Unlike other labeling ligands specific only to certain types of glioma cells, CTX is a unique peptide which can specifically target the vast majority of glioma tumors with MMP-2 as the receptor.[6] Typically, CTX-I^{131} conjugates have already been used in phase I/II clinical trials for tagging gliomas in surgical resection.[8] Conjugates based on CTX and fluoresceins such as dyes,[9, 10] quantum dots,[6] and rare-earth nanoparticles[11] have also been presented to trace gliomas *in vitro* and *in vivo*. In addition, CTX can also act as an effective inhibitor with significant therapeutic potential for the diseases that regulates the activity of MMP-2.[9] It has been reported that CTX conjugated iron oxide nanoparticles can inhibit the glioma cell invasion via MMP-2.[12] Furthermore, CTX fusion protein with N-terminal Polyhistidine tag (his6)[8,14] and Glutathione S-transferase tagged (GST)[13] have also exhibited the ability to selectively bind the gliomas and inhibit the cancer cell invasion.

On the other hand, noble metal nanoclusters (NCs) (e.g., Au) have been regarded promising fluorescent agents for medical bioimaging due to their low toxicity, bright fluorescence, as well as ultrasmall particle size (usually less than 2 nm) in comparison with other commonly used nanoparticles. Especially, these ultrasmall particles will be benefit for glioma imaging across the blood-brain barrier (BBB).[14-16] There are several methods for synthesizing fluorescent Au NCs have been reported.[17-29] Among them, one important kind of method involves the usage of biomolecules such as dendrimers,[18-21] proteins,[22-28] and DNA[29] as templates to synthesize the Au NCs. The introduction of biomolecules in the synthesis of Au NCs can make the procedure

green and the products capped with biomolecules show increased biocompatibility to living species.

In this work, we employ CTX fusion protein GST-CTX (gCTX) as a template to direct the synthesis of the Au NCs at the physiological temperature (37 °C). The resulting Au@gCTX NCs not only have intense red fluorescence maximized at 620 nm, but also retain the bioactivity of the gCTX to label the gliomas and inhibit the tumor proliferation and MMP-2 activity. Cellular uptake studies, Gelatin Zymography, MTT cell viability assay, and flow cytometry have been performed to assess their ability to act as robust theranostic agents to glioma treatment.

Results and Discussion

Physicochemical characterization of Au@gCTX NCs

The CTX nucleotide sequence was generated from the natural CTX peptide by an overlapping PCR method (see Table 1). The recombinant gCTX protein was cloned, expressed and purified by the strategy reported by our group previously.[11] The synthesis process of the Au@gCTX NCs was similar to the biomineralization behavior of organisms in nature.[26] As the functional template, the CTX fusion protein (gCTX) sequestered and interacted with the gold ions, and provided scaffolds for cluster formation (see Fig. 1a). Through adjusting the pH to ~12, the entrapped ions underwent progressive reduction to form Au NCs in situ. The Au NCs were stabilized within CTX fusion protein as the Au@gCTX NCs.

High resolution transmission electron microscopy (HRTEM) is utilized to investigate the morphology of the Au@gCTX NCs. As shown in Fig. 1b, the Au@gCTX NCs are appeared to be spheres in shape and homogeneously distributed with size of approximately 2.0 nm. Their hydrodynamic diameter was further measured by Dynamic Light Scattering (DLS). As shown in Fig. 1c, the average hydrodynamic diameter of the Au@gCTX NCs is only 2.2 nm, which is just a little larger than the size observed through the HRTEM, suggesting that the Au@gCTX NCs have very good dispersibility in water solution. These results confirm that Au NCs possess an ultrasmall particle size.[27, 28]

The oxidation state of the Au@gCTX NCs is determined by X-ray photoelectron spectroscopy (XPS). A shown in Fig. 1d, the observed binding energy values for Au NCs show Au $4f_{7/2}$ ~83.5 eV and Au $4f_{5/2}$ ~87.2 eV, which are blue-shifted in comparison with those of Au^{3+} (86.3 eV and 89.4 eV).[22] It indicates that most of the Au ions have been reduced to the Au atoms.

The Fourier transform infrared spectroscopy (FTIR) spectra of the gCTX and Au@gCTX NCs are shown in Fig. 1e. The characteristic amide I band at 1670 $cm^{-1}$is as expected for a protein with a high proportion of α-helix. The band appearing at 1446 cm^{-1} is attributed to the strong primary amine scissoring, whereas the band centered at 3430 cm^{-1} is attributed to the primary amines. The band appearing at 2929 cm^{-1} corresponds to C-H vibration. It can be observed that the FTIR characteristics of the gCTX and Au@gCTX NCs are almost same. This finding indicates that no modification of the surface electric property of the gCTX has occurred in the synthesis of the Au@gCTX NCs.

Optical properties of Au@gCTX NCs

The optical properties of the Au@gCTX NCs are displayed in Fig. 2. Under a ultraviolet (UV) light irradiation, the deep brown

Table 1 The primers of overlapping PCR for the synthesis of CTX gene.

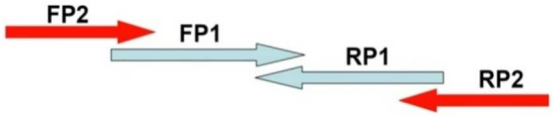

Name	Sequence(5'-3')
FP1	CGTAAATGTGACGATTGCTG TGGTGGCAAAGGTCGTGGTA AATGCTACGG
FP2	GCC**GGATCC**CCGATGACGAT GACAAAATGTGTATGCCGTG CTTCACTACC
RP1	CAATCGTCACATTTACGTGC CATCTGGTGATCGGTAGTGA AGCACGGCAT
RP2	GCC**CTCGAG**TCAACGGCACA GACACTGCGGACCGTAGCAT TTACCACGAC

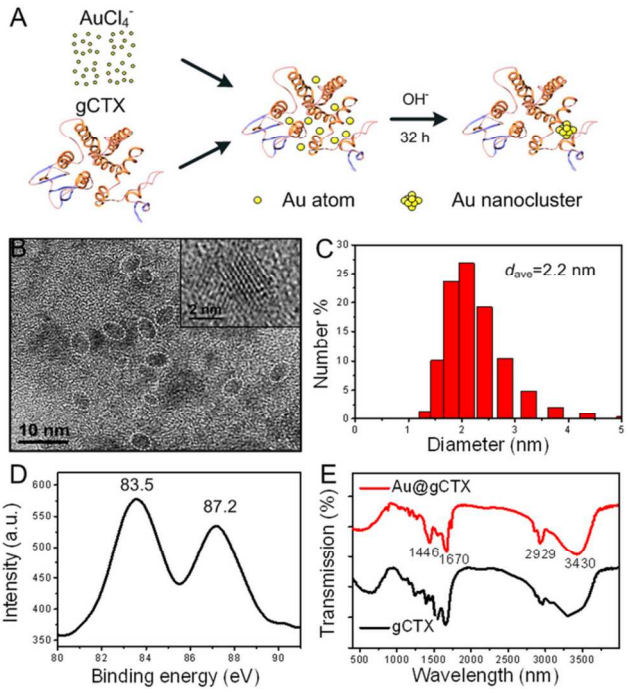

Fig. 1 (a) Schematic of the formation of Au@gCTX NCs. (b, c, d) HRTEM image (b), DLS histogram(c), and XPS data (d) of Au@gCTX NCs. (e) FTIR spectra of Au@gCTX NCs and gCTX powders.

solution of the Au@gCTX NCs emitintense red fluorescence.In contrast, the free gCTX solution show weak blue fluorescence, which is characteristic of the aromatic side groups in the amino acid residues.[30] Under a370 nm light excitation, the Au@gCTX NCs exhibit one emission peaked at approximately 620 nm, while the free gCTX shows no such emission. The quantum yield of the Au@gCTX NCs has been determined by using rhodamine as the reference. It is found that their quantum yield is approximately 6.5%, which is a little higher than the Au@BSA NCs synthesized using the same method.[26] The photostability of the Au@gCTX NCs is further tested. When the water solution of the Au@gCTX NCs is continually exposed to a 375 nm Xe lamp for over 1 h, no reduction can be found in the emission intensity, demonstrating their good photostability.

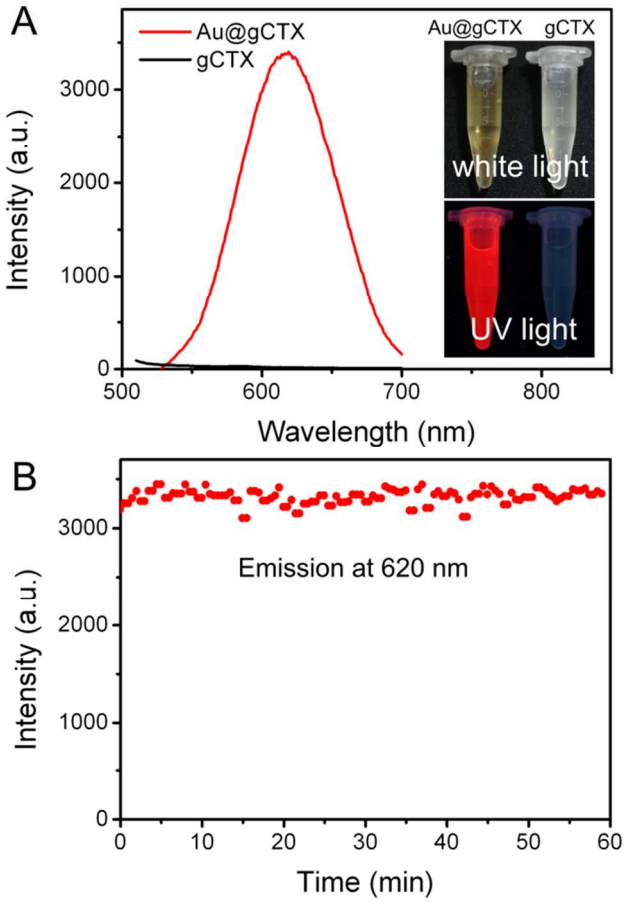

Fig. 2(a) Emission spectra (λ_{ex}=370 nm) of Au@gCTX NCs. The inset is the photographs of the solutions of Au@gCTX NCs and gCTX under white light (up) and UV light (down) irradiation. (b) Photostability test of Au@gCTX NCs under a 375 nm light excitation for 60 min.

The gel electrophoresis experiments of the Au@gCTX NCs have been performed by using the Au@BSA NCs as the control sample (see Fig. 3). DNA Marker and DNA (Lane M and Lane 1) has been used to verify the agarose gel system. The aqueous $HAuCl_4$ (Lane 2), BSA (Lane 3) and gCTX (Lane 4), which are the raw materials in the nanocluster synthesis, show no fluorescence under the UV light irradiation. In contrast, the Au@BSA NCs (Lane 5) and Au@gCTX NCs (Lane 6) exhibit bright fluorescence. It can be observed that the Au@gCTX NCs move faster than the Au@BSA NCs in the gel electrophoresis. The bright fluorescence of the Au@gCTX NCs further confirms that the Au NCs have successfully been trapped in the gCTX protein.

Specific imaging of cancer cells with Au@gCTX NCs

To investigate the targeting ability of the Au@gCTX NCs to glioma cells, three sets of cell imaging experiments were performed (see Fig. 4). One experimental group was set as to exploit the positive absorbance, a negative group trial and a competitive group trial were set as controls. First of all, C6 glioma cells were treated with the Au@gCTX NCs and Au@BSA NCs, which were set as the targeted specificity group and non-specific group, respectively. In another set of experiment, a competed experiment was used as a further proof to

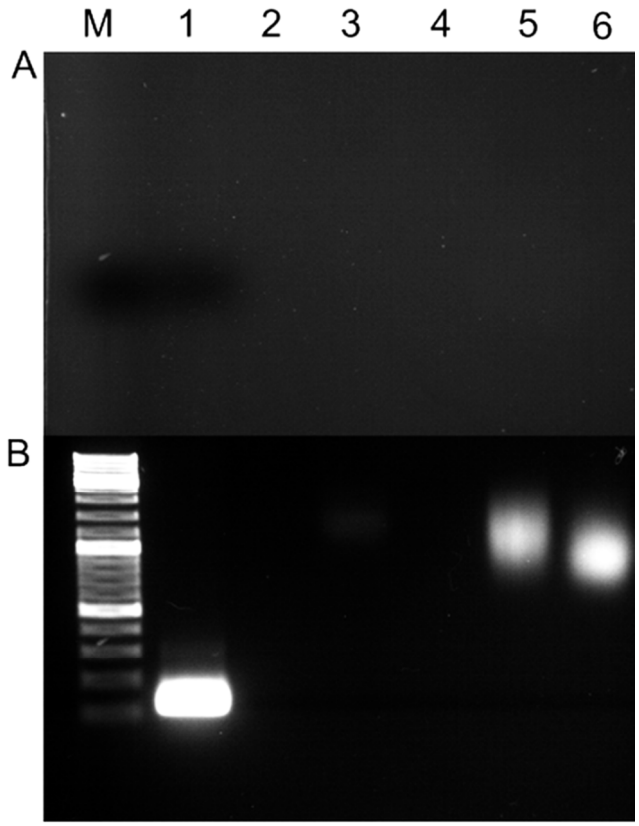

Fig. 3 Agarose gel electrophoresis of Au@gCTX NCs under white light (a) and UV light (b) irradiation. The samples added in the lane from left to right are as the followings: M: DNA Marker; 1: DNA (140bp); 2: $HAuCl_4$; 3: BSA; 4: gCTX; 5: Au@BSA NCs; 6: Au@gCTX NCs.

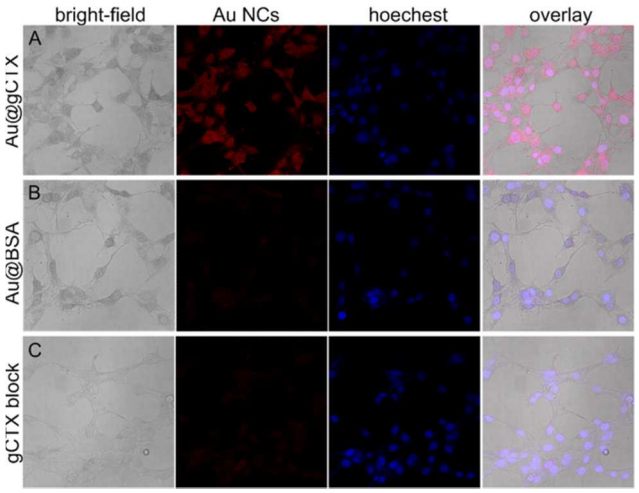

Fig. 4 Confocal fluorescent microscopy imaging in C6 glioma cells with Au@gCTX NCs(a), Au@BSA NCs(b),and Au@gCTX NCs with 5 times fold molar excess gCTX(c).

illuminate the gCTX-mediated target delivery by treating the same batch of C6 cells with both the Au@gCTX NCs and 5 times fold molar excess free gCTX.

As shown in Fig. 4, the bright-field images, red fluorescence images, dark-field blue fluorescence images of nucleus, and the overlay images are presented from left to right. Fig.4a shows the result of the Au@gCTX NCs targeted group, which clearly exhibit that bright red fluorescence surrounded the blue nucleus

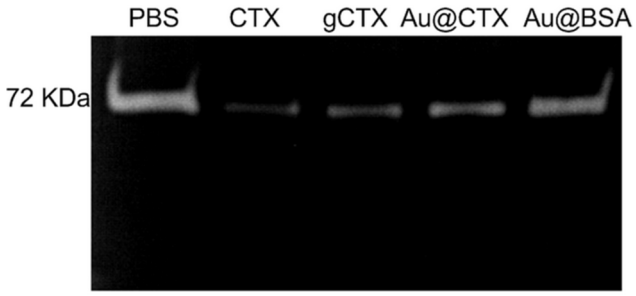

Fig. 5 Gelatin Zymography about MMP-2 activity ofC6 glioma cells, which were treated with (1) PBS, (2) CTX peptide, (3) gCTX protein, (4) Au@gCTX NCs, and (5) Au@BSA NCs.

in the C6 cells, indicating that some of the Au@gCTX NCs have crossed the cell membrane and entered into the cytoplasm, and some have accumulated near the perinuclear region. Fig. 4b shows the result of C6 glioma cells incubated with the Au@BSA NCs, showing very low red fluorescence, which may be nonspecific uptake in nature. Fig. 4c shows the result of the competitive test by using 5 times fold molar excess free gCTX. It can be observed that almost no fluorescence in the C6 cells can be observed, which demonstrate that the specific binding of the Au@gCTX NCs was competitively inhibited. These results indicate that the Au@gCTX NCs can target C6 glioma cells with high specificity. It is well known that CTX is a chloride channel blocker[31] to bind specifically to MMP-2 associated with the channels.[9] The MMP-2 is reported to be upregulated in many types of cancer, which appeared to be a correlation between the level of MMP-2 expression and poor outcome of the disease.[32-38] Therefore, the Au@gCTX NCs may also be specific to other cancer with high level of MMP-2 expression.

Inhibitory capability to MMP-2 activity

It is known that CTX and gCTX have remarkable anti-invasive effect for gliomas by reducing MMP-2 expression on glioma cell membranes and suppressing the proteolytic activity of MMP-2 through binding to MMP-2.[9-11, 39-41] Here, the inhibitory effect of the Au@gCTX NCs to the MMP-2 activity is tested by using Gelatin Zymography (see Fig. 5). The blank control C6 cell line shows a high level of MMP-2 activity in the conditioned medium after starvation culture (Line 1). The CTX peptide and gCTX fusion protein significantly inhibit the secretory MMP-2 activity as the positive controls (Line 2 and Line 3, respectively). Similar to the positive controls, the Au@gCTX NCs also inhibit the secretory MMP-2 activity (Line 4), but the Au@BSA NCs do not present obvious inhibitory activity (Line 5). These results demonstrate that the Au@gCTX NCs retain the bioactivity of gCTX, and have the similar inhibitory capability of secretory MMP-2 activity as the gCTX.[42] It suggests that the Au@gCTX NCs can interact with this entire protein complex which is correlated with tumor invasion, neovascularization, and metastasis of gliomas.

Inhibitory capability to glioma cell growth

MTT assay is used to investigate the inhibitory capability of the Au@gCTX NCs to the C6 glioma cell proliferation (see Fig. 6a). The C6 cells were incubated for 24 h with medium containing various concentrations (60, 170, 500, 1500 μg/mL) of the

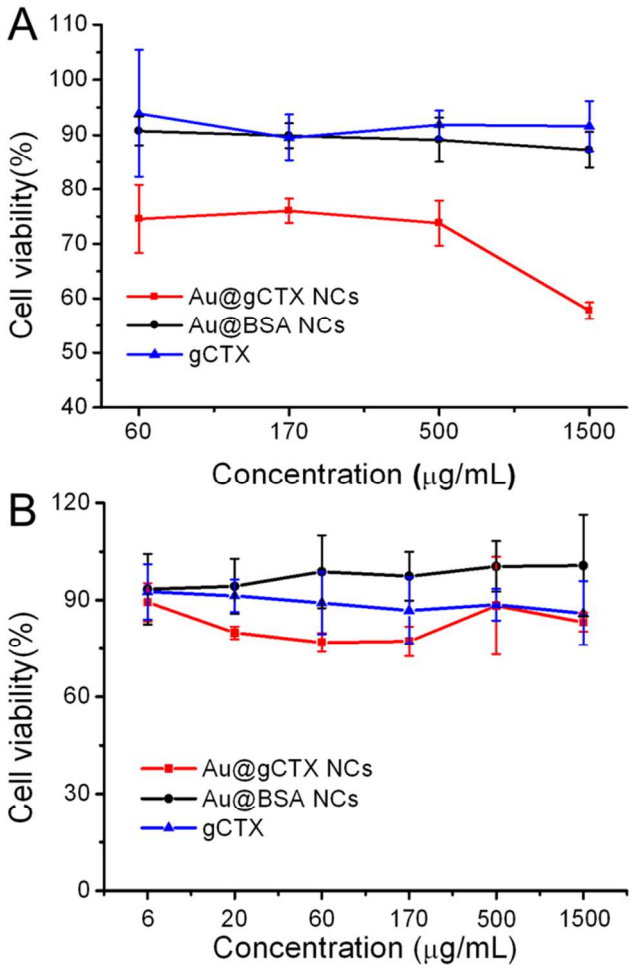

Fig. 6 *In vitro* viability of C6 glioma cells (a) and normal NIH3T3 cells(b) treated with Au@gCTX NCs, Au@BSA NCs, and free gCTX protein at 60, 170, 500, 1500 μg/mL of protein for 24 h incubation.

Au@gCTX NCs, and the Au@BSA NCs and free gCTX protein were employed as controls. It can be observed that the Au@gCTX NCs efficiently inhibit the growth of the C6 glioma cells with the inhibition rate of 42.23 ± 1.51%, while the Au@BSA NCs and free gCTX with the same concentration show no such effect. The MTT assay results suggest that the Au@gCTX NCs have the cytostatic activity, which can shift cancer cells from proliferation to quiescence.[43, 44]

The cytotoxicity of the Au@gCTX NCs, Au@BSA NCs and free gCTX protein to normal cells was further tested by incubating them with NIH 3T3 cells for 24 h (see Fig. 6b). Similar with the Au@BSA NCs and free gCTX protein, the Au@gCTX NCs are not toxic to NIH 3T3 cells even at the high concentration of 1500 μg/mL, which is the concentration can efficiently inhibit the C6 glioma cell proliferation. It demonstrates that the Au@gCTX NCs can specifically inhibit cancer cell proliferation without harmful to normal cells.

In addition to the MTT assay, the reactive oxygen species (ROS) in the C6 glioma cells treated with the Au@gCTX NCs is further evaluated by using FACS, and the Au@BSA NCs and PBS are employed as controls. It is known that oxidative stress is one of the most important mechanisms governing cell death due to

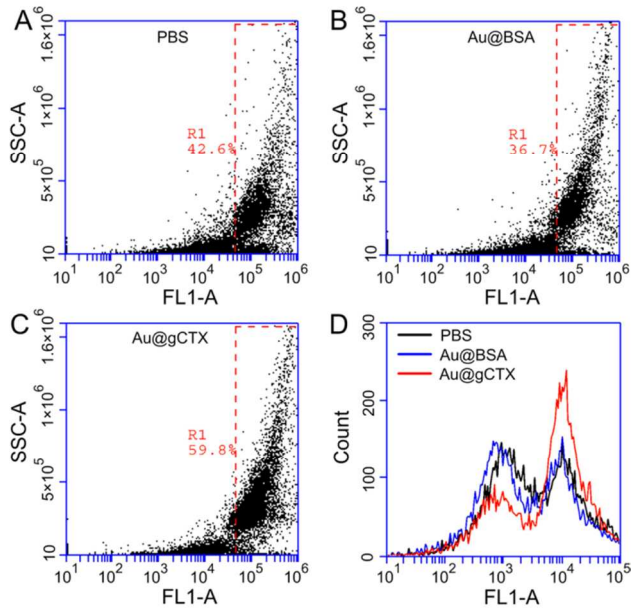

Fig. 7(a-c) Intracellular ROS generation assay by using DCFH-DA to show the proportion of generating ROS in the C6 glioma cells treated with PBS (a), Au@BSA NCs (b), and Au@gCTX NCs (c)at 1500 μg/mL of protein for 48h incubation. (d) Intensity of fluorescence curves of C6 glioma cells treated with PBS, Au@BSA NCs, and Au@gCTX NCs

nanomaterial-mediated toxicity.[45] The overproduction of ROS can lead to oxidative stress in cellular systems via a variety of stimuli that surpass the capacity of the intracellular antioxidant defense system, resulting in the damage of the cellular components.[46] In our experiments, DCFH-DA, a reduced form of fluorescein has been used to load with the C6 cells. Because DCFH-DA can be converted into its fluorescent form via the cleavage of acetate groups by intracellular esterasesor oxidation, the ROS levels of the C6 cells can be analyzed by flow cytometry. As shown in Fig. 7, the intracellular ROS level of the C6 cells treated with the Au@gCTX NCs is 59.8%, while both the Au@BSA NCs and PBS result in very low intracellular ROS level. The results demonstrate that the elevated ROS levels are involved to the C6 cell death caused by the Au@gCTX NCs. The enhanced intracellular oxidative stress is probably ascribed to the catalytic activity of the Au NCs to the oxidation reactions,[47] which can intervene in the biological antioxidant defense responses, induce the mitochondrial membrane permeability, and damage the respiratory chain to trigger the apoptotic process, thereby inhibit the cell proliferation.[46, 48, 49]

Conclusions

In conclusion, an ultrasmall and cancer-specific theranostic agent with bright fluorescence and excellent gCTX bioactivity has successfully been prepared by using the gCTX as a template to direct the synthesis of the Au@gCTX NCs. The *in vitro* studies demonstrate their ability to not only trace the cancer cells with high specificity but also inhibit the enzymatic activity of MMP-2 and cancer proliferation by elevating intracellular ROS levels, without harmful to normal cells. These findings suggest an efficient method for the synthesis of multifunctional theranostic agent for the treatment of cancer.

Acknowledgements

The authors acknowledge financial support from the National Basic Research Program of China (973 program # 2011CB933600), National Natural Science Foundation of China (grant No # 81071249, 20875062, 20905050, 10874134), Guangdong Innovation Research Team of Low-cost Healthcare, and Science and Technology Key Project of Shenzhen (JC201104220242A).

Notes and references

[a] *Guangdong Key Laboratory of Nanomedicine, CAS Key Lab of Health Informatics, Institute of Biomedicine and Biotechnology, Shenzhen Institutes of Advanced Technology, Chinese Academy of Sciences, Shenzhen 518055, China.*

[b] *State Key Laboratory of Virology, College of Life Sciences, Wuhan University, Wuhan 430072, PR China.*

**Corresponding authors. Tel.: 86 755-86392210; Fax: 86 755-86392299. E-mail addresses:xf.yu@siat.ac.cn (X.-F. Yu), lt.cai@siat.ac.cn (L. Cai), wxli@whu.edu.cn (W. Li).*

1. M. F. Kircher, U. Mahmood, R. S. King, R. Weissleder and L. Josephson, *Cancer Res*, 2003, **63**, 8122-8125.
2. Y. Tao, M. Ning and H. Dou, *Nanomedicine*, 2013, **9**, 222-232.
3. S. Y. Tzeng and J. J. Green, *Ther Deliv*, 2013, **4**, 687-704.
4. R. Qiao, Q. Jia, S. Huwel, R. Xia, T. Liu, F. Gao, H. J. Galla and M. Gao, *ACS Nano*, 2012, **6**, 3304-3310.
5. A. M. Smith and S. Nie, *Nat Biotechnol*, 2009, **27**, 732-733.
6. R. L. Orndorff and S. J. Rosenthal, *Nano Lett*, 2009, **9**, 2589-2599.
7. H. S. Choi, W. Liu, P. Misra, E. Tanaka, J. P. Zimmer, B. Itty Ipe, M. G. Bawendi and J. V. Frangioni, *Nat Biotechnol*, 2007, **25**, 1165-1170.
8. A. N. Mamelak, S. Rosenfeld, R. Bucholz, A. Raubitschek, L. B. Nabors, J. B. Fiveash, S. Shen, M. B. Khazaeli, D. Colcher, A. Liu, M. Osman, B. Guthrie, S. Schade-Bijur, D. M. Hablitz, V. L. Alvarez and M. A. Gonda, *J Clin Oncol*, 2006, **24**, 3644-3650.
9. J. Deshane, C. C. Garner and H. Sontheimer, *J Biol Chem*, 2003, **278**, 4135-4144.
10. M. Veiseh, P. Gabikian, S. B. Bahrami, O. Veiseh, M. Zhang, R. C. Hackman, A. C. Ravanpay, M. R. Stroud, Y. Kusuma, S. J. Hansen, D. Kwok, N. M. Munoz, R. W. Sze, W. M. Grady, N. M. Greenberg, R. G. Ellenbogen and J. M. Olson, *Cancer Res*, 2007, **67**, 6882-6888.
11. X. F. Yu, Z. Sun, M. Li, Y. Xiang, Q. Q. Wang, F. Tang, Y. Wu, Z. Cao and W. Li, *Biomaterials*, 2010, **31**, 8724-8731.
12. O. Veiseh, J. W. Gunn, F. M. Kievit, C. Sun, C. Fang, J. S. Lee and M. Zhang, *Small*, 2009, **5**, 256-264.
13. S. Fan, Z. Sun, D. Jiang, C. Dai, Y. Ma, Z. Zhao, H. Liu, Y. Wu, Z. Cao and W. Li, *Cancer Lett*, 2010, **291**, 158-166.
14. A. B. Etame, C. A. Smith, W. C. Chan and J. T. Rutka, *Nanomedicine*, 2011, **7**, 992-1000.
15. D. T. Wiley, P. Webster, A. Gale and M. E. Davis, *Proc Natl Acad Sci U S A*, 2013, **110**, 8662-8667.
16. J. Frigell, I. Garcia, V. Gomez-Vallejo, J. Llop and S. Penades, *J Am Chem Soc*, 2014, **136**, 449-457.
17. J. Zheng, P. R. Nicovich and R. M. Dickson, *Annu Rev Phys Chem*, 2007, **58**, 409-431.
18. H. Duan and S. Nie, *J Am Chem Soc*, 2007, **129**, 2412-2413.
19. Y. P. Bao, H. C. Yeh, C. Zhong, S. A. Ivanov, J. K. Sharma, M. L. Neidig, D. M. Vu, A. P. Shreve, R. B. Dyer, J. H. Werner and J. S. Martinez, *J Phys Chem C*, 2010, **114**, 15879-15882.
20. H. Kawasaki, H. Yamamoto, H. Fujimori, R. Arakawa, Y. Iwasaki and M. Inada, *Langmuir*, 2010, **26**, 5926-5933.
21. S. Fukuzumi, R. Hanazaki, H. Kotani and K. Ohkubo, *J Am Chem Soc*, 2010, **132**, 11002-11003.
22. Y. Negishi, K. Nobusada and T. Tsukuda, *J Am Chem Soc*, 2005, **127**, 5261-5270.
23. B. Adhikari and A. Banerjee, *Chem-Eur J*, 2010, 16, 13698-13705.

24. H. Kawasaki, K. Hamaguchi, I. Osaka and R. Arakawa, *Adv Funct Mater*, 2011, **21**, 3508-3515.
25. M. A. Habeeb Muhammed, P. K. Verma, S. K. Pal, A. Retnakumari, M. Koyakutty, S. Nair and T. Pradeep, *Chemistry*, 2010, **16**, 10103-10112.
26. J. Xie, Y. Zheng and J. Y. Ying, *J Am Chem Soc*, 2009, 131, 888-889.
27. C. Y. Shao, B. Yuan, H. Q. Wang, Q. Zhou, Y. L. Li, Y. F. Guan and Z. X. Deng, *J Mater Chem*, 2011, **21**, 19413-19413.
28. R. Ghosh, A. K. Sahoo, S. S. Ghosh, A. Paul and A. Chattopadhyay, *Acs Appl Mater Inter*, 2014, **6**, 3822-3828.
29. G. Y. Lan, W. Y. Chen and H. T. Chang, *Analyst*, 2011, 136, 3623-3628.
30. C.-L. Liu, H.-T. Wu, Y.-H. Hsiao, C.-W. Lai, C.-W. Shih, Y.-K. Peng, K.-C. Tang, H.-W. Chang, Y.-C. Chien, J.-K. Hsiao, J.-T. Cheng and P.-T. Chou, *Angew Chem Int Ed Engl*, 2011, **50**, 7056-7060.
31. J. A. DeBin, J. E. Maggio and G. R. Strichartz, *Am J Physiol*, 1993, **264**, C361-369.
32. L. Bello, V. Lucini, G. Carrabba, C. Giussani, M. Machluf, M. Pluderi, D. Nikas, J. Zhang, G. Tomei, R. M. Villani, R. S. Carroll, A. Bikfalvi and P. M. Black, *Cancer Res*, 2001, **61**, 8730-8736.
33. Y. Itoh, A. Takamura, N. Ito, Y. Maru, H. Sato, N. Suenaga, T. Aoki and M. Seiki, *EMBO J*, 2001, **20**, 4782-4793.
34. C. M. Overall, E. Tam, G. A. McQuibban, C. Morrison, U. M. Wallon, H. F. Bigg, A. E. King and C. R. Roberts, *J Biol Chem*, 2000, **275**, 39497-39506.
35. Z. Kachra, E. Beaulieu, L. Delbecchi, N. Mousseau, F. Berthelet, R. Moumdjian, R. Del Maestro and R. Beliveau, *Clin Exp Metastasis*, 1999, **17**, 555-566.
36. A. Pagenstecher, A. K. Stalder, C. L. Kincaid, S. D. Shapiro and I. L. Campbell, *Am J Pathol*, 1998, **152**, 729-741.
37. J. Decock, W. Hendrickx, H. Wildiers, M. R. Christiaens, P. Neven, M. Drijkoningen and R. Paridaens, *Clin Exp Metastasis*, 2005, **22**, 495-502.
38. U. W. Nilsson, S. Garvin and C. Dabrosin, *Breast Cancer Res Treat*, 2007, **102**, 253-261.
39. S. J. Pan, S. K. Zhan, B. G. Pei, Q. F. Sun, L. G. Bian and B. M. Sun, *Int J Immunopathol Pharmacol*, 2012, **25**, 871-881.
40. Y. Fu, N. An, K. Li, Y. Zheng and A. Liang, *Journal of Neuro-Oncology*, 2011, **107**, 457-462.
41. C. Qin, B. He, W. Dai, H. Zhang, X. Wang, J. Wang, X. Zhang, G. Wang, L. Yin and Q. Zhang, *Mol Pharm*, 2014.
42. N. Pal, T. Yamamoto, G. F. King, C. Waine and B. Bonning, *Toxicon*, 2013, **70**, 114-122.
43. H. P. Berridge MV, and Tan AS, *Biotech Annu Rev*, 2005, **11**, 127-152.
44. T. Mosmann, *J Immunol Methods*, 1983, **65**, 55-63.
45. K. Krishnamoorthy, M. Veerapandian, L. H. Zhang, K. Yun and S. J. Kim, *J Phys Chem C*, 2012, **116**, 17280-17287.
46. M. Premanathan, K. Karthikeyan, K. Jeyasubramanian and G. Manivannan, *Nanomedicine*, 2011, **7**, 184-192.
47. X. Nie, H. Qian, Q. Ge, H. Xu and R. Jin, *ACS Nano*, 2012, **6**, 6014-6022.
48. T. Xia, M. Kovochich, J. Brant, M. Hotze, J. Sempf, T. Oberley, C. Sioutas, J. I. Yeh, M. R. Wiesner and A. E. Nel, *Nano Lett*, 2006, **6,** 1794-1807.
49. Q. Xie, G. Lan, Y. Zhou, J. Huang, Y. Liang, W. Zheng, X. Fu, C. Fan and T. Chen, *Cancer Lett*, 2014, **354**, 58-67.